CMS Physics Analysis Summary

Contact: cms-pag-conveners-exotica@cern.ch 2016/03/11

Search for leptophobic Z' decaying into four leptons in the final state at $\sqrt{s} = 8$ TeV

The CMS Collaboration

Abstract

A search for heavy narrow resonances decaying into four-lepton final states in events that contain no identified $Z \to \ell^+\ell^-$ decays has been performed with an integrated luminosity of 19.7 fb^{-1} of proton-proton collision data at $\sqrt{s} = 8$ TeV collected by the CMS experiment. No excess of events over the standard model expectation is observed. Upper limits for a model-independent scenario and comparison with the predictions of a benchmark model on the fiducial cross section times branching fraction for the production of these heavy narrow resonances are presented.

1 Introduction

A new heavy neutral gauge boson, Z', is predicted in extensions of the standard model (SM) based on an extra Abelian gauge group $U(1)'$, including Grand Unified Theories (GUTs) [1, 2], Randall-Sundrum graviton models and Kaluza-Klein excitation of extra dimensions [3, 4]. Searches for Z' resonances at hadron colliders are usually performed using the dijet [5], lepton-antilepton [6, 7] and top-antitop [8] final states. The dilepton channel provides a large cross section and a very clean signal compared to the dijet or $\mathrm{t\bar{t}}$ channels. However, if the Z' does not couple to the SM leptons, the dilepton search will be unsuccessful. Although searches based on the dijet final state remain sensitive, they suffer from large QCD dijet backgrounds.

We extend the search for heavy neutral vector bosons to include possible Z' decays into particles predicted by various models from beyond the SM (BSM) theories, in addition to the SM modes. In this paper we present an analysis searching for a leptophobic Z' resonance that decays into 4 leptons from cascade decays of the Z'. One example benchmark model is described in Ref. [9]. Such a baryonic gauge boson is motivated in order to protect the proton from decay and can be produced with a large cross section at the LHC. These non-typical Z' resonances decay into a pair of new scalar bosons (Φ) with the Φs decaying subsequently into two leptons (e or μ). Fig. 1 shows the 4-lepton Z' resonance diagram at an hadron collider. Contribution of Φ decaying into τs are not considered in this paper.

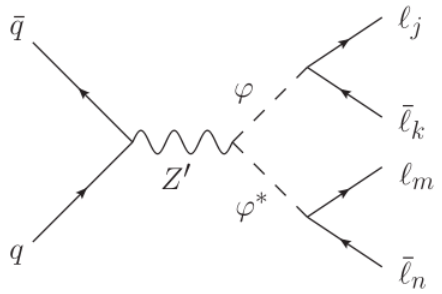

Figure 1: four-lepton Z' resonance diagram at a hadron collider [9].

The analysis is a signature-based search for heavy narrow resonances decaying into four isolated leptons in the final state. The following four-lepton final states are considered: $\mu\mu\mu\mu$, $\mu\mu\mu e$, $\mu\mu ee$, μeee, $eeee$. In particular, $\mu\mu\mu e$ and μeee are included to allow for lepton flavor violation [10–12] in the decays of the new scalar bosons. All couplings of Φ are assumed to be equal to $ee, \mu\mu, e\mu$ in the lepton flavor violation channels. The benchmark model assumes narrow ($\Gamma/M < 1\%$) natural width of Z'. Our detector resolution effect is generally much larger than the width of Z' in all channels. Events with identified $Z \to \mu^+\mu^-$ and $Z \to \mathrm{e}^+\mathrm{e}^-$ decays are vetoed in order to suppress the dominant ZZ background. The search described in this paper is designed to be independent of the details of specific Z' models, and limits on the fiducial cross sections times branching fraction of the four-lepton production are set. Additionally the results are interpreted in the context of the benchmark model [9].

2 CMS detector

The central feature of the CMS apparatus is a superconducting solenoid of 6 m internal diameter, providing a magnetic field of 3.8 T. Within the superconducting solenoid volume are a silicon pixel and strip tracker, a lead tungstate crystal electromagnetic calorimeter (ECAL), and a brass and scintillator hadron calorimeter (HCAL), each composed of a barrel and two endcap

sections. Muons are measured in gas-ionization detectors embedded in the steel flux-return yoke outside the solenoid. Extensive forward calorimetry complements the coverage provided by the barrel and endcap detectors.

The electromagnetic calorimeter consists of 75 848 lead tungstate crystals which provide coverage in pseudorapidity $|\eta| < 1.479$ in a barrel region (EB) and $1.479 < |\eta| < 3.0$ in two endcap regions (EE). A preshower detector consisting of two planes of silicon sensors interleaved with a total of $3X_0$ of lead is located in front of the EE. The electron momentum is estimated by combining the energy measurement in the ECAL with the momentum measurement in the tracker. The momentum resolution for electrons with $p_T \approx 45$ GeV from $Z \to e^+e^-$ decays ranges from 1.7% for nonshowering electrons in the barrel region to 4.5% for showering electrons in the endcaps [13].

Muons are measured in the pseudorapidity range $|\eta| < 2.4$, with detection planes made using three technologies: drift tubes, cathode strip chambers, and resistive plate chambers. Matching muons to tracks measured in the silicon tracker results in a relative transverse momentum resolution for muons with $20 < p_T < 100$ GeV of 1.3–2.0% in the barrel and better than 6% in the endcaps. The p_T resolution in the barrel is better than 10% for muons with p_T up to 1 TeV [14]. A more detailed description of the CMS detector, together with a definition of the coordinate system used and the relevant kinematic variables, can be found in Ref. [15].

3 Event selection

The full 2012 dataset corresponding to an integrated luminosity of 19.7 fb^{-1} of proton-proton collision data at $\sqrt{s} = 8$ TeV is used for this analysis. The data are collected with inclusive lepton triggers with various p_T thresholds. The trigger used for the muon-enriched channels ($\mu\mu\mu\mu, \mu\mu\mu e$) requires the presence of at least one muon candidate with $p_T > 40$ GeV and $|\eta| < 2.1$. The trigger used for the electron-enriched channels ($\mu eee, eeee$) requires two clusters in the ECAL with transverse energy $E_T > 33$ GeV. For the $\mu\mu ee$ channel, muon-photon cross trigger with a $p_T > 22$ GeV for both objects is required.

The signal Monte Carlo (MC) sample for the benchmark model was produced using the CalcHep 3.4.1 generator interfaced with PYTHIA v6.4.24 [16, 17]. The sample is divided into five decay channels ($\mu\mu\mu\mu, \mu\mu\mu e, \mu\mu ee, \mu eee, eeee$) for different Z' masses ranging from 250 GeV to 3000 GeV in increments of 250 GeV. The Φ mass is varied between 5%, 10%, 20%, 30% and 40% of the Z' mass with an additional fixed point of 50 GeV. The benchmark model assumes that no new particles besides the Z' and the Φ will be heavy enough to affect the production and decay of the Z' boson. The leading order (LO) signal cross section times branching fraction ranges in each channel as follows: $\mu\mu\mu\mu$ and $eeee$ $(0.77 - 3.0 \times 10^{-6})$pb, $\mu\mu ee$ $(2.30 - 1.1 \times 10^{-5})$ pb, and $\mu\mu\mu e$ and μeee $(1.53 - 4.5 \times 10^{-5})$ pb for the mass range used in this analysis (250 GeV to 3000 GeV). These MC samples were used to optimize event selection, evaluate signal efficiencies and calculate exclusion limits.

Various SM MC samples are used to estimate the backgrounds. The dominant background is the production of ZZ decaying into four leptons. The qq-induced ZZ production was generated using the PYTHIA event generator and the gg-induced production using GG2ZZ program [17, 18]. Additional backgrounds from diboson production (WW, WZ) were generated with PYTHIA and top production ($t\bar{t}$, tW, $\bar{t}W$) were generated with POWHEG [19]. Other processes like $t\bar{t}Z$ and triboson production ($WW\gamma$, WWZ, WZZ, ZZZ) were generated with MADGRAPH rescaled by NLO k-factors [20]. All MC samples were generated using the CTEQ6L parton distribution functions (PDFs) set and the PYTHIA Z2 tune in order to model the proton

structure and the underlying event [21, 22]. The samples were then processed with the full CMS detector simulation software based on GEANT4, which includes trigger simulation and the CMS event reconstruction [23].

Events are required to contain at least one offline reconstructed primary vertex (PV) with at least four tracks associated to the vertex and its r and z coordinates are required to be within 2 and 24 cm of the nominal interaction point. Two leading leptons are required to have $p_{\mathrm{T}} > 45$ GeV and two sub-leading leptons $p_{\mathrm{T}} > 30$ GeV and all four leptons must be in $|\eta| < 2.4$.

Muon candidates are reconstructed either by a combined fit including hits in both tracker and muon detectors (global muon) or as tracks in the tracker matched to track segments in the muon system (tracker muons) [14]. The global muons are required to pass the following criteria: at least one pixel hit, at least six strip tracker layers, at least one muon chamber hit, at least two muon stations with the muon segments, a transverse impact parameter of the tracker track $|d_{xy}| < 0.2$ cm with respect to the PV, longitudinal distance of the tracker track $|d_z| < 0.5$ cm with respect to the PV, and $\delta p_{\mathrm{T}}/p_{\mathrm{T}} < 0.3$. To take into account the boosted signature, if two muons are as close as $\Delta R < 0.4$, where the $\Delta R = \sqrt{\Delta\phi^2 + \Delta\eta^2}$, one of the muons is allowed to be reconstructed only as a tracker muon. All muon candidates are required to be isolated. Muons are considered isolated if the scalar sum of all track p_{T}'s, except identified muon candidates, within a cone of $\Delta R < 0.3$ around the muon does not exceed 10% of the their p_{T}.

Electron candidates are built by matching clusters in ECAL to groups of hits in silicon pixel detector which are then used as a seed for track reconstruction in the tracker [24]. A set of identification criteria is required to suppress jet misidentified as electrons. Electrons are required to pass the following criteria: the profile of energy deposition in the ECAL be consistent with the expectation of the electron, the sum of HCAL energy deposits be less than 10% of the electron's ECAL energy, and the track associated with the cluster have no more than one hit missing in the pixel layers and the transverse impact parameter $|d_{xy}| < 0.02$ cm with respect to the primary vertex associated with the candidates.

If the electron pairs are heavily boosted, as it is often the case in the searched signal events, they can be easily merged into one cluster in ECAL. The probability to find a merged electron pair in benchmark signal MC sample with $M(Z') = 3$ TeV and $M(\Phi_{ll}) = 50$ GeV is estimated to be about 50%. Therefore, electron candidates having $E_{\mathrm{T}} > 500$ GeV, the ratio of ECAL cluster energy to track momentum larger than 1.5 and a second track with $p_{\mathrm{T}} > 30$ GeV within the cone of $\Delta R(\mathrm{track}, \mathrm{electron}) < 0.25$, are considered to be merged electron pairs. All electron candidates are required to be isolated using the following definition: the sum of the p_{T} of all other tracks in a cone of $\Delta R < 0.3$ around the track of the electron candidate is required to be less than 5 GeV and the sum of the E_{T} of the energy deposits in the calorimeter that are not associated with the candidate is required to be less than 5% of the candidate E_{T} [7]. This is softer than the isolation requirement of 3% in Ref. [7] because the latter introduces a non-negligible inefficiency in our analysis (approximately 6% at electron E_{T} = 1 TeV). In addition, we remove the contribution of the second electron if it is close in both the p_{T} sum of tracks and the sum of the E_{T} of energy deposits.

Events with two oppositely charged same-flavor leptons with $89 < M_{ll} < 93$ GeV are rejected in this analysis. The requirement is designed to suppress dominant ZZ background with almost no signal efficiency loss for M(Z′) > 500 GeV. The mass window should be as narrow as possible in order to avoid degradation of the signal efficiency. More than 70% (30%) ZZ background is rejected by the veto requirement additionally in muon (electron) channel. The difference between two channels is caused by the merged electron treatment in the electron channel. As described above, if the single electron is identified as the merged electron then

it is treated as a dielectron pair and the invariant mass of the merged electron can not be reconstructed. Hence the veto requirement is not applied to the merged electron and the power of the veto requirement is weakened in the electron channel. A typical event efficiency is 50–70% ($\mu\mu\mu\mu$), 55–65% ($\mu\mu\mu e$ and $\mu\mu ee$) and 45–65% (μeee and $eeee$) throughout the entire mass range at M(Φ_{ll}) = 50 GeV. The other M(Φ_{ll}) scenarios, M(Φ_{ll}) = 5%, 10%, 20%, 30%, and 40% of M(Z'), have less significant boosted signature and therefore they have higher efficiency than the M(Φ_{ll}) = 50 GeV scenario. The efficiency for the other M(Φ_{ll}) samples is approximately 10–15% (1–5%) higher in electron (muon) channels depending on the mass range than M(Φ_{ll}) = 50 GeV scenario.

4 Background estimation

Most of the SM backgrounds are suppressed by the requirement of four isolated high quality leptons. The dominant backgrounds are ZZ events decaying into four leptons. Other background comes from top events with two genuine leptons and two lepton candidates arising from misidentified jets. WW (WZ) also can pass the event selection if they contain two (one) fake or non-prompt leptons from jets and similarly in the triboson productions. These small backgrounds were estimated using MC simulation.

Contribution from events in which more than two leptons arise from misidentified jets is expected to be very small because this analysis requires four isolated leptons in the final state. This background originated from the misidentification is estimated using so-called "fake rate" method described in Ref. [7]. The fake rate measured as a function of electron E_{T} in the barrel and endcap is applied to fake electron enriched events. The contribution from jet backgrounds estimated using this procedure is found to be negligible.

Fig. 2 shows the four-lepton invariant mass distributions (M_{4l}) for selected events. The MC predictions are normalized using the integrated luminosity and higher order theoretical cross sections (NNLO for $\mathrm{t\bar{t}}$ [25] and NLO for others described above). The data is in good agreement with the expected SM backgrounds in all channels.

The observed events and estimated backgrounds are summarized in Table 1. As shown in the table, the observed events are in good agreement with the expected backgrounds. The number of expected backgrounds from SM processes in the region ($M > 1$ TeV) is less than one event.

Channel	100 GeV $< M <$ 1 TeV					$M >$ 1 TeV	
	N_{obs}	SM backgrounds				N_{obs}	N_{tot}
		N_{ZZ}	N_{top}	N_{EW}	N_{tot}		
$Z' \to \mu\mu\mu\mu$	3	4.9 ± 0.3	0.9 ± 0.5	—	5.9 ± 0.6	0	—
$Z' \to \mu\mu\mu e$	6	0.4 ± 0.1	1.3 ± 0.6	1.2 ± 0.3	2.9 ± 0.7	0	—
$Z' \to \mu\mu ee$	12	9.3 ± 0.4	3.0 ± 1.5	1.2 ± 0.3	13.5 ± 1.6	0	0.1 ± 0.1
$Z' \to \mu eee$	2	0.2 ± 0.1	0.4 ± 0.1	0.6 ± 0.2	1.2 ± 0.2	0	0.1 ± 0.1
$Z' \to eeee$	9	15.0 ± 0.5	0.2 ± 0.1	0.2 ± 0.1	15.4 ± 0.5	0	0.2 ± 0.1
combination	32	29.9 ± 0.7	5.7 ± 1.9	3.3 ± 0.5	38.9 ± 2.1	0	0.4 ± 0.2

Table 1: Summary of observed yield and expected backgrounds for all channels, where N_{obs} is the number of observed events in the data. The total backgrounds (N_{tot}) are sum of three different backgrounds estimated using MC simulation: N_{ZZ} is ZZ background, N_{top} is backgrounds from $\mathrm{t\bar{t}}$, single top and ttZ, and N_{EW} is backgrounds from WW and WZ and triple gauge coupling processes. Errors are statistical uncertainty only.

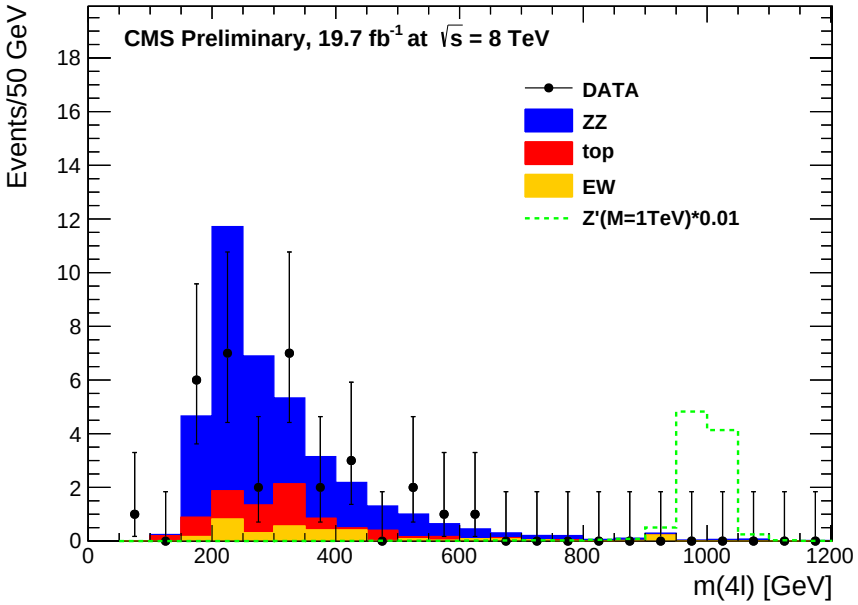

Figure 2: The four-lepton invariant mass spectrum for the combination of the five studied channels. The points with error bars represent the data; the histograms represent the expectations from SM processes. "top" denotes the sum of the events for $t\bar{t}$, tW, $\bar{t}$W, ttZ and "EW" denotes the sum of the events from WW, WZ, WWγ, WWZ, WZZ and ZZZ. Dashed (green) histogram shows the expectation from the benchmark signal model at M = 1 TeV with $M(\Phi_{ll}) = 50$ GeV scaled down by a factor 100.

5 Results

No excess of events in data is observed compared to the SM predictions. Exclusion limits are calculated with a Bayesian approach at 95% confidence level (C.L.) in both the model-independent way and in the context of the benchmark model. The signal fiducial region (100 GeV $< M(Z') <$ 3 TeV) consists of four leptons (e or μ) with $|\eta| < 2.4$: two leading leptons are required to have $p_{\mathrm{T}} > 45$ GeV and two sub-leading leptons are required to have $p_{\mathrm{T}} > 30$ GeV. Within this fiducial region, we measure the event selection efficiency using the benchmark signal model. Signal MC samples with $M(\Phi_{ll}) = 50$ GeV are used for the efficiency calculation, which demonstrate the worst scenario of the boosted signature in the final state. The efficiencies for each channel are fairly stable with respect to the invariant mass, slightly decrease at highest mass. The likelihood function is defined as:

$$L(\mathrm{data}|\theta,\vec{\nu}) = \prod_{\mathrm{channels}} Poisson(\mathrm{data}|\theta,\vec{\nu}) \cdot p(\vec{\nu}) \quad (1)$$

where θ is the signal strength modifier, p is the prior probability, $\vec{\nu}$ is the full set of nuisance parameters that are used to incorporate systematic uncertainties. The systematic uncertainties of luminosity, backgrounds, and event selection efficiency are included in the nuisance parameters for the limit calculation with a Markov chain. This method is based on interpreting the likelihood as a probability distribution with a set of PDFs for the nuisance parameters, which are treated with the Log-normal parametrization. Integrating over the nuisance parameters we find the limit for the signal strength. Table 2 shows the results of the limit calculations.

Channel	$\mathcal{L}$ (fb^{-1})	ϵ_i	$\sigma_i^{\text{4l fid}} \cdot Br_i$ (fb)
$eeee$	19.7 ± 0.5	0.45 ± 0.10	0.38
μeee		0.47 ± 0.10	0.37
$\mu\mu ee$		0.51 ± 0.10	0.34
$\mu\mu\mu e$		0.52 ± 0.10	0.34
$\mu\mu\mu\mu$		0.55 ± 0.10	0.32

Table 2: Limits at 95% C.L. on the product of cross section and branching fraction for the five studied channels. $\mathcal{L}$ is the integrated luminosity, ϵ_i is the selection efficiency for each channel (obtained using M(Z') = 3 TeV benchmark signal MC samples), $i = eeee, \mu eee, \mu\mu ee, \mu\mu\mu e, \mu\mu\mu\mu$, $\sigma^{\text{4l fid}}$ is the cross section in the fiducial region, an Br is the branching fraction.

Systematic uncertainties on the muon selection including reconstruction, identification and isolation are 0.5% [14]. The uncertainties on the electron selection are 0.7% (0.6%) for electrons below 100 GeV in EB(EE) and 1.4% (0.4%) for electrons above 100 GeV in EB(EE) [7]. The uncertainties due to the lepton efficiency on both signal and background events in five studied channels vary between 2.2% and 2.7% as a function of four lepton invariant mass and 10% uncertainty is assigned totally for each channel, including the effect of the boosted signature. The impact of uncertainty in the electron energy scale on signal (backgrounds) is 1% (0.5%) [7]. Uncertainties on the muon momentum scale and mass resolutions are below 0.1% [14]. 30% uncertainty for background cross section (ZZ and $t\bar{t}$) is used to take into account effects from the PDFs and higher order QCD corrections. The uncertainty on the integrated luminosity is assigned to be 2.6% [26]. In this analysis, the statistical uncertainties are dominant and the systematic uncertainties have small impact on the results. We tested the sensitivity of the obtained limits by assigning two times larger uncertainties and observed only a negligible change in the calculated limits. Hence we conclude that the obtained results are not very sensitive to variations of the systematic uncertainties.

Limits on the product of cross section and branching fraction are set in the context of the benchmark model as a function of the four-lepton invariant mass. Mass resolution of the detector is generally larger than the natural width of the Z' resonance in all channels. In the limit calculation, we set up the mass window to be six times the mass resolution centered around the signal mass point considered. A counting experiment is performed for the limit calculation in this analysis. Fig. 3 shows the limits on the cross section times branching fraction. Top left plot shows the limit of the lepton flavor conserved (LFC) channels ($eeee$ + μeee + $\mu\mu\mu\mu$), top right plot of the lepton flavour violated (LFV) channels (μeee + $\mu\mu\mu e$) and bottom plot of all five studied channels. In this benchmark model, the hypothesis is that different channels have the same branching fraction. The black solid (dotted) line indicates the observed (expected) 95% C.L., the green (yellow) band indicates the $\pm 1(2)\ \sigma$ uncertainty, and the blue dotted line shows the theoretical Z' cross section for M(Φ_{ll}) = 50 GeV. This theoretical cross section is calculated under an assumption that the $Br(\Phi \to 2l) = 100\%$, where $l = e$ or μ. The bands are not visible above 1–1.5 TeV mass regions because backgrounds are negligible in the region. The 95% C.L. limit on the mass of a baryonic Z' resonance is 2.4 TeV(LFC), 2.2 TeV(LFV), and 2.5 TeV (combined). Table 3 shows the exclusion region in the M(Φ_{ll}) vs M(4l) plane for all five channels. The two-dimensional limit is calculated using the benchmark signal samples with 6 different M(Φ_{ll}) scenarios including the event selection efficiencies. The theoretical prediction of cross sections decreases if Φ has higher mass, and also boosted signature will be less significant in the case (and efficiency is increased accordingly). Therefore the other scenarios, M(Φ_{ll}) = 5%, 10%, 20%, 30%, and 40% of M(Z'), have slightly lower results for the limits than M(Φ_{ll}) = 50 GeV scenario as shown in the table.

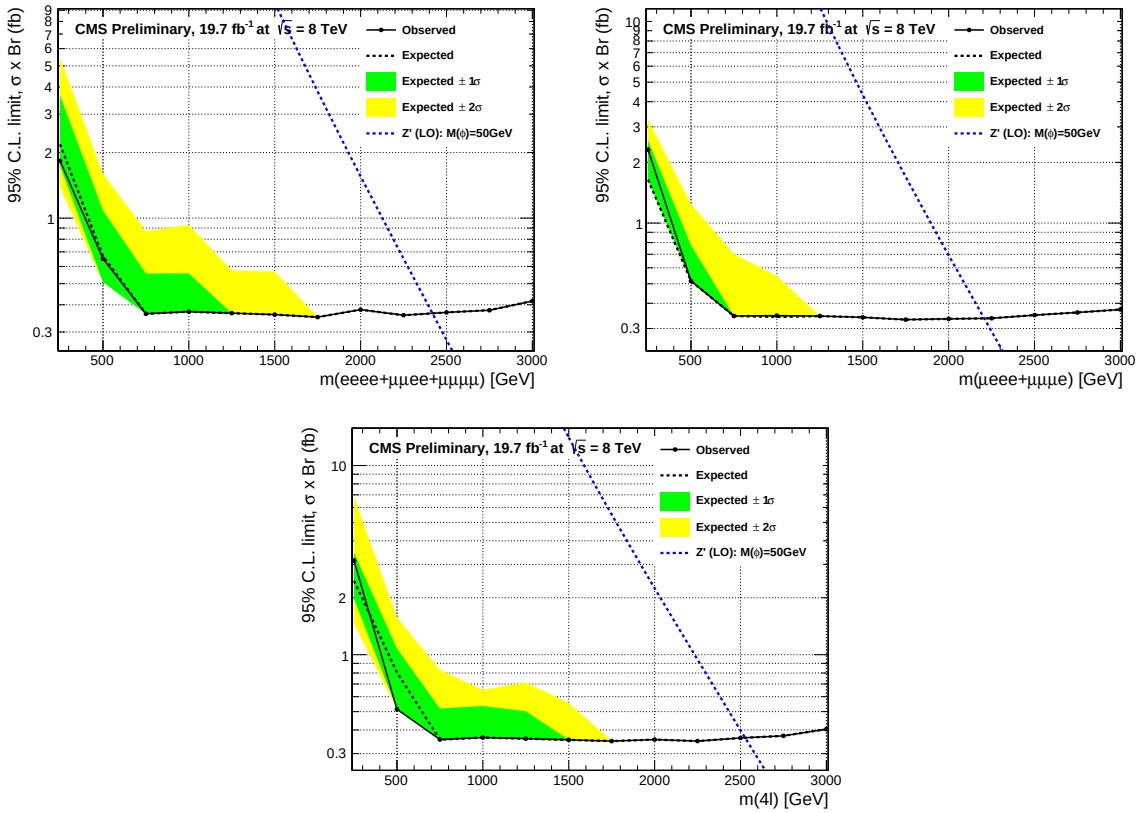

Figure 3: The 95% C.L. upper limit on the cross section times branching fraction as a function of the four lepton invariant mass for the combination of the LFC conserved channels (top left), the LFV channels (top right), and all five studied channels (bottom). Shaded green (yellow) band indicates the one and two sigma uncertainty bands on the expected limits. The blue dotted line represents the theoretical predictions for M(Φ_{ll}) = 50 GeV.

M(Φ_{ll})	50 GeV	5% of M(Z')	10% of M(Z')	20% of M(Z')	30% of M(Z')	40% of M(Z')
eeee	1.6 TeV	1.7 TeV	1.7 TeV	1.7 TeV	1.7 TeV	1.7 TeV
μeee	2.0 TeV	1.8 TeV	1.9 TeV	1.9 TeV	1.9 TeV	1.9 TeV
μμee	2.4 TeV	1.9 TeV	2.0 TeV	2.0 TeV	2.0 TeV	2.0 TeV
μμμe	2.0 TeV	1.8 TeV	1.9 TeV	1.9 TeV	1.9 TeV	1.9 TeV
μμμμ	1.7 TeV	1.6 TeV	1.7 TeV	1.7 TeV	1.7 TeV	1.7 TeV
LFV	2.2 TeV	2.0 TeV	2.1 TeV	2.1 TeV	2.1 TeV	2.1 TeV
LFC	2.4 TeV	2.1 TeV	2.1 TeV	2.1 TeV	2.1 TeV	2.1 TeV
combined	2.5 TeV	2.3 TeV	2.3 TeV	2.3 TeV	2.3 TeV	2.3 TeV

Table 3: The 95% C.L. limit calculation in the M(Φ_{ll}) vs M(4l) plane for each channel and for the combination of all channels. It is evaluated using the benchmark signal MC samples with six different scenarios (M(Φ_{ll}) = 50 GeV and 5%, 10%, 20%, 30%, and 40% of M(Z')).

6 Summary

This paper presents a search for heavy narrow resonances decaying into four-lepton final states using proton-proton collisions data at $\sqrt{s} = 8$ TeV corresponding to an integrated luminosity of 19.7 fb^{-1}. The four-lepton invariant mass spectra in all considered channels are consistent with SM predictions. 95% C.L. limits on the the model-independent fiducial cross section times branching fraction are calculated. In addition exclusion limits for a specific benchmark model with various M(Φ_{ll}) scenarios are calculated. A model-independent limits are in the range of 0.32–0.38 fb depending on the channel. A Z' in the benchmark model can be excluded below 2.5 TeV in the combination of the five studied channels for M(Φ_{ll}) = 50 GeV, and the exclusion region on the M(Φ_{ll}) vs M(4l) plane is determined.

References

[1] A. Leike, "The phenomenology of extra neutral gauge bosons", *Phys. Rept.* **317** (1999) 143, doi:10.1016/S0370-1573(98)00133-1, arXiv:9805494.

[2] J. L. Hewett and T. G. Rizzo, "Low-energy phenomenology of superstring-inspired E6 models", *Phys. Rept.* **183** (1989) 193, doi:10.1016/0370-1573(89)90071-9.

[3] L. Randall and R. Sundrum, "An alternative to compactification", *Phys. Rev. Lett.* **83** (1999) 4690, doi:10.1103/PhysRevLett.83.4690, arXiv:9906064.

[4] L. Randall and R. Sundrum, "A large mass hierarchy from a small extra dimension", *Phys. Rev. Lett.* **83** (1999) 3370, doi:10.1103/PhysRevLett.83.3370, arXiv:9905221.

[5] CMS Collaboration, "Search for narrow resonances using the dijet mass spectrum in pp collisions at sqrt(s) = 8 TeV", *Phys.Rev.* **D87** (2013) 114015, doi:10.1103/PhysRevD.87.114015, arXiv:1302.4794.

[6] CMS Collaboration, "Search for heavy narrow dilepton resonances in pp collisions at $\sqrt{s} = 7$ TeV and $\sqrt{s} = 8$ TeV", *Phys. Lett. B* **720** (2013) 63–82, doi:10.1016/j.physletb.2013.02.003, arXiv:1212.6175.

[7] CMS Collaboration, "Search for physics beyond the standard model in dilepton mass spectra in proton-proton collisions at $\sqrt{s} = 8$ TeV", *JHEP* **04** (2015) 025, doi:10.1007/JHEP04(2015)025, arXiv:1412.6302.

[8] CMS Collaboration, "Search for anomalous t t-bar production in the highly-boosted all-hadronic final state", *JHEP* **1209** (2012) 029, doi:10.1007/JHEP09(2012)029, arXiv:1204.2488.

[9] V. Barger and H.-S. Lee, "Four-lepton resonance at the Large Hadron Collider", *Phys. Rev. D* **85** (2012) 055030, doi:10.1103/PhysRevD.85.055030.

[10] Y. Kuno and Y. Okada, "Muon decay and physics beyond the standard model", *Reviews of Modern Physics* **73** (2001) 151.

[11] A. de Gouvea and P. Vogel, "Lepton Flavor and Number Conservation and Physics Beyond the Standard Model", arXiv:1303.4097.

[12] D. K. Ghosh, P. Roy, and S. Roy, "Four lepton flavor violating signals at the LHC", *JHEP* **05** (2012) 067.

[13] CMS Collaboration, "Performance of electron reconstruction and selection with the CMS detector in proton-proton collisions at $\sqrt{s} = 8$ TeV", *JINST* **10** (2015) P06005, doi:10.1088/1748-0221/10/06/P06005, arXiv:1502.02701.

[14] CMS Collaboration, "Performance of CMS muon reconstruction in pp collision events at $\sqrt{s} = 7$ TeV", *JINST* **7** (2012) P10002, doi:10.1088/1748-0221/7/10/P10002, arXiv:1206.4071.

[15] CMS Collaboration, "The CMS experiment at the CERN LHC", *JINST* **3** (2008) S08004, doi:10.1088/1748-0221/3/08/S08004.

[16] A. Belyaev, N. Christensen, and A. Pukhov, "CalcHEP 3.4 for collider physics within and beyond the Standard Model", *Computer Physics Communications* **184** (2013) doi:10.1016/j.cpc.2013.01.014, arXiv:1207.6082.

[17] T. Sjöstrand, S. Mrenna, and P. Z. Skands, "PYTHIA 6.4 physics and manual", *JHEP* **05** (2006) 026, doi:10.1088/1126-6708/2006/05/026, arXiv:hep-ph/0603175.

[18] T. Binoth, N. Kauerm, and P. Mertsch, "Gluon-induced QCD corrections to $pp \to ZZ \to l\bar{l}l'\bar{l}'$", arXiv:0807.0024.

[19] S. Alioli, P. Nason, C. Oleari, and E. Re, "NLO vector-boson production matched with shower in POWHEG", *JHEP* **07** (2008) 060, doi:10.1088/1126-6708/2008/07/060, arXiv:0805.4802.

[20] J. Alwall et al., "MadGraph v5: going beyond", *JHEP* **06** (2011) 128, doi:10.1007/JHEP06(2011)128, arXiv:1106.0522.

[21] J. Pumplin et al., "New Generation of Parton Distributions with Uncertainties from Global QCD Analysis", *JHEP* **07** (2002) 012, doi:10.1088/1126-6708/2002/07/012, arXiv:0201195.

[22] R. Field, "Min-Bias and the Underlying Event at the LHC", *Acta Phys. Polon. B* **42** (2011) 2631, doi:10.5506/APhysPolB.42.2631, arXiv:1202.0901.

[23] GEANT4 Collaboration, "GEANT4—a simulation toolkit", *Nucl. Instrum. Meth. A* **506** (2003) 250, doi:10.1016/S0168-9002(03)01368-8.

[24] CMS Collaboration, "Electron Reconstruction and Identification at $\sqrt{s} = 7$ TeV", *CMS Physics Analysis Summary CMS-PAS-EGM-10-004* (2010).

[25] M. Czakon, P. Fiedler, and A. Mitov, "Total Top-Quark Pair-Production Cross Section at Hadron Colliders Through O(α_S^4)", *Phys. Rev. Lett.* **110** (2013) 252004, doi:10.1103/PhysRevLett.110.252004, arXiv:1303.6254.

[26] CMS Collaboration, "CMS Luminosity Based on Pixel Cluster Counting - Summer 2013 Update", CMS Physics Analysis Summary CMS-PAS-LUM-13-001, 2013.